Journal of Statistical Physics, Vol. 86, Nos. 5/6, 1997

Corner Exponents in the Two-Dimensional Potts Model

Dragi Karevski,[1] Peter Lajkó,[1,2] and Loïc Turban[1]

Received May 14, 1995; final July 16, 1996

The critical behavior at a corner in two-dimensional Ising and three-state Potts models is studied numerically on the square lattice using transfer operator techniques. The local critical exponents for the magnetization and the energy density for various opening angles are deduced from finite-size scaling results at the critical point for isotropic or anisotropic couplings. The scaling dimensions compare quite well with the values expected from conformal invariance, provided the opening angle is replaced by an effective one in anisotropic systems.

KEY WORDS: Potts model; corner exponents; anisotropy; length rescaling.

1. INTRODUCTION

The surface shape of a system may have some influence on its local critical behavior at a second order phase transition. This was shown by Cardy[1] for a magnetic system with $O(N)$ symmetry within mean-field theory and in $d=4-\varepsilon$ dimensions. The local magnetic exponent at a wedge was found to vary continuously with the opening angle θ.

Marginal behavior was also obtained at a corner in the two-dimensional Ising model using the star–triangle recursion relation on the triangular lattice and the corner-to-corner spin correlation function on the square lattice to calculate the corner magnetization.[2,3] The same problem was later studied on the square lattice using row-to-row[4] or corner[5]

[1] Laboratoire de Physique du Solide (URA CNRS No 155), Université Henri Poincaré (Nancy I), F-54506 Vandœuvre lès Nancy Cedex, France.

[2] Permanent address: Department of Theoretical Physics, University of Szeged, H-6720 Szeged, Hungary.

0022-4715/97/0300-1153$12.50/0

822/86/5-6-17

transfer matrix techniques. An expression for the 90° corner magnetization was conjectured in ref. 4. Recently, Abraham and Latrémolière[6, 7] obtained the edge magnetization analytically, as a function of the distance from the corner, thus confirming the conjecture of Kaiser and Peschel.

Other systems were also considered, such as the planar Heisenberg antiferromagnet[8] and the self-avoiding walk confined into a wedge in two and three dimensions.[9-13]

In two dimensions a varying corner exponent $x^c(\theta)$ immediately follows from the conformal mapping $w = z^{\theta/\pi}$ which transforms the half-plane into a wedge with opening angle θ.[14, 2] The decay of the critical corner-to-bulk correlation functions then gives

$$x^c(\theta) = \frac{\pi}{\theta} x^s \tag{1.1}$$

where x^s is the corresponding surface exponent. This result is valid for isotropic systems only. When the couplings are anisotropic, lengths have to be rescaled in order to restore isotropy[1, 2] and (1.1) still applies with an effective value of the opening angle.

The marginal local critical behavior may be understood by considering a system with a "parabolic" shape, $y = \pm Cx^{\alpha}$.[15, 16] Under a length rescaling by a factor b, C transforms into $C' = b^{\alpha - 1}C$. Thus the flow is toward the flat surface geometry when $\alpha > 1$ and toward the half-line when $\alpha < 1$. When $\alpha = 1$, i.e., for the corner geometry, the surface shape is scale invariant and $C = \tan(\theta/2)$ is the marginal variable.

Up to now, the conformal result (1.1) has been checked for the local magnetic exponent $x_m^c(\theta)$ with opening angles corresponding to simple fractions of π. In the present work, we extend these results by studying the local critical behavior of both the energy and the magnetization in the two-dimensional q-state Potts model with $q = 2, 3$. Various rational values of $\tan(\theta/2)$ and $\tan\theta$ are considered. In Section 2 we use a local operator formalism for the construction of the row-to-row transfer matrices which are needed for the corner geometry on a square lattice. The corner exponents are deduced from a finite-size scaling analysis of the data for isotropic and anisotropic systems in Section 3.

2. POTTS MODEL IN THE CORNER GEOMETRY

We consider the zero-field Potts model with Hamiltonian

$$-\beta\mathcal{H} = \sum_{i,j} [K_1(q\delta_{\sigma(i,j),\sigma(i+1,j)} - 1) + K_2(q\delta_{\sigma(i,j),\sigma(i,j+1)} - 1)] \tag{2.1}$$

where δ is the Kronecker delta function and the Potts variables $\sigma(i, j)$ take the values 0, 1,..., $q-1$. When $q=2$, the Ising model is recovered. The sum runs over the bonds of a square lattice in the corner geometry as shown in Fig. 1. The couplings are assumed to be anisotropic with values K_1 in the vertical direction and K_2 in the horizontal one.

Let us define the row-to-row transfer matrix elements as

$$T_{m,m-1} = \langle m | T_m | m-1 \rangle$$
$$= \exp\left[K_1 \sum_{j=n(m)}^{N(m)} (q\delta_{\sigma_j, \sigma_j'} - 1) + K_2 \sum_{j=n(m)}^{N(m)-1} (q\delta_{\sigma_j, \sigma_{j+1}} - 1) \right] \quad (2.2)$$

where $\sigma_j(\sigma_j')$ denote the Potts variables on the mth $[(m-1)$th$]$ row, respectively. $|m\rangle$ is a state vector corresponding to a configuration of the Potts variables from $n(m)$ to $N(m)$ along the mth row and T_m is the transfer operator acting on this state vector.

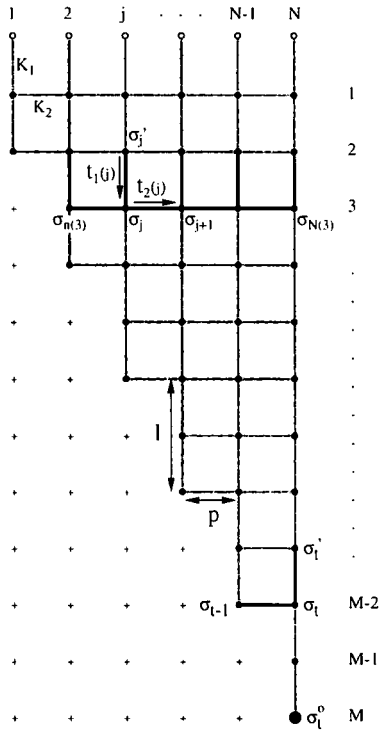

Fig. 1. Corner geometry and transfer operator.

The transfer operator can be written as the product $T_m = V_2(m)\, V_1(m)$ with[17]

$$V_1(m) = \exp\left[K_1^* \sum_{j=n(m)}^{N(m)} \sum_{p=1}^{q-1} (R_j)^p \right]$$
$$V_2(m) = \exp\left[K_2 \sum_{j=n(m)}^{N(m)-1} \sum_{p=1}^{q-1} (C_j^\dagger C_{j+1})^p \right] \tag{2.3}$$

K_1^* is a dual coupling such that $x_1 x_1^* = q$ with $x_i = \exp(qK_i) - 1$. The operator C_j is diagonal on the basis of the Potts states $|\sigma_j\rangle$, whereas R_j acts as a ladder operator on the same basis, so that

$$C_j |\sigma_j\rangle = \exp\left(i \frac{2\pi}{q} \sigma_j \right) |\sigma_j\rangle, \qquad (R_j)^p |\sigma_j\rangle = |\sigma_j + p\rangle \qquad (\mathrm{mod}\ q) \tag{2.4}$$

Introducing local transfer operators

$$t_1(j) = x_1 + \sum_{p=0}^{q-1} (R_j)^p, \qquad t_2(j) = 1 + \frac{x_2}{q} \sum_{p=0}^{q-1} (C_j^\dagger C_{j+1})^p \tag{2.5}$$

we have that, up to an unimportant constant factor, the row-to-row transfer operator appearing in (2.2) can be rewritten as

$$T_m = \prod_{j=n(m)}^{N(m)-1} t_2(j) \prod_{j=n(m)}^{N(m)} t_1(j) \tag{2.6}$$

This transfer operator may be viewed as a discrete time evolution operator acting on the Potts state vector at time $m-1$ to make it evolve to its state at time m. Due to the corner geometry, this operator is time dependent. Given an initial state $|i\rangle$ at time 0, corresponding to the top edge in Fig. 1, this state will evolve to

$$|m\rangle = T_m T_{m-1} \cdots T_2 T_1 |i\rangle \tag{2.7}$$

at time m. In the sequel we shall use either free or fixed boundary conditions on the top edge. Fixed boundary conditions correspond to an initial state $|k\rangle = |\sigma_1 \sigma_2 \cdots \sigma_N\rangle$, whereas for free boundary conditions one has to take a superposition $|f\rangle = q^{-N/2} \sum_{k=1}^{q^N} |k\rangle$ of the q^N configurations of the N Potts variables with equal amplitudes. One may notice in Fig. 1 that a site variable σ_j with $j < n(m)$ or $j > N(m)$ remains frozen at time m and later.

The corner magnetization m_c is calculated with the Potts variable σ_t^0, where t is the index of the column corresponding to the tip (see Fig. 1). It is given by[18]

$$m_c = \frac{q\langle \delta_{\sigma_t^0,0}\rangle - 1}{q-1}, \qquad \langle \delta_{\sigma_t^0,0}\rangle = \frac{1}{q}\sum_{p=0}^{q-1} \frac{\langle f|\, C_t^p\, |M\rangle}{\langle f|M\rangle} \tag{2.8}$$

where the average of the Kronecker delta follows from (2.4). The state $|f\rangle$ corresponds to free boundary conditions on the sides of the wedge, whereas $|M\rangle$ is defined as in (2.7) with $|i\rangle = |00\cdots 0\rangle$. Thus the top edge is fixed with all the sites in the state 0. At the critical point this symmetry-breaking boundary condition ensures that the tip magnetization remains nonvanishing on a finite system.

The energy density associated with a bond can be defined, up to a constant factor, as the average of the Kronecker delta. When the bond is horizontal, the system evolves as above up to time $M-2$, where the value of $\delta_{\sigma_{t-1},\sigma_t}$ is taken (see Fig. 1), and the corner energy density is given by

$$e_c^h = \langle \delta_{\sigma_{t-1},\sigma_t}\rangle = \frac{1}{q}\sum_{p=0}^{q-1} \frac{\langle f|\, T_M T_{M-1}(C_{t-1}^{\dagger} C_t)^p\, |M-2\rangle}{\langle f|M\rangle} \tag{2.9}$$

With a vertical bond one obtains nonvanishing contributions to the average of the Kronecker delta when there is no flip along this bond, so that $t_1(t)$ in (2.5) contributes a factor $1+x_1$. With the geometry of Fig. 1 the energy density can be written as

$$e_c^v = \langle \delta_{\sigma_t,\sigma_t'}\rangle = (1+x_1)\frac{\langle f|\, T_M T_{M-1} \prod_j t_2(j) \prod_{j\neq t} t_1(j)\, |M-3\rangle}{\langle f|M\rangle} \tag{2.10}$$

These expressions are easily generalized for other shapes.

3. NUMERICAL RESULTS

The Potts exponents for the corner magnetization and the corner energy density have been obtained through finite-size scaling at the critical point for different opening angles, using the shapes sketched in Fig. 2. In order to limit the size N of the system, we use only unit steps ($p=1$) in the horizontal direction and change the angle θ by varying l (see Fig. 1). The maximum sizes studied are $N=19$ for $q=2$ (Ising model) and $N=11$ for $q=3$, so that an extrapolation of the finite-size estimates of the exponents is needed. Isotropic and anisotropic sytems have been considered.

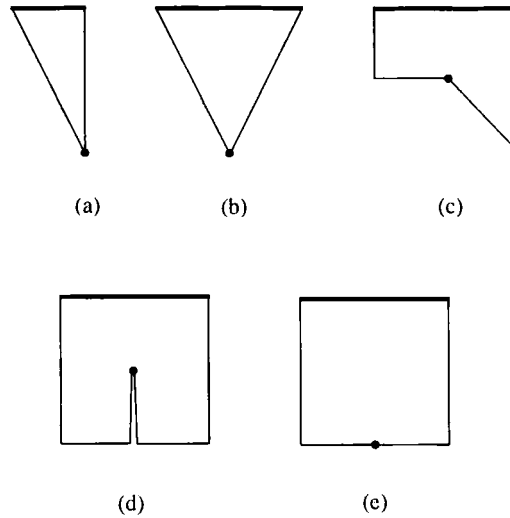

Fig. 2. The different system shapes used to calculate the corner magnetization and energy density. The Potts states at the top edge (bold line) are either fixed or free.

When the system is isotropic the critical point, corresponding to $x_1 x_2 = q$, is located at $K_c = (1/q) \ln(1 + \sqrt{q})$. The critical corner magnetization decays as

$$m_c^{\text{crit}}(N) = A_m(\theta)\, N^{-x_m^c}$$

with the system size N.

The corner exponent $x_m^c(\theta)$ deduced from sequence extrapolations of the finite-size estimates using the BST algorithm[19] is given in Table I. The numerical results are in quite good agreement with the values expected from conformal invariance in Eq. (1.1) with the surface magnetic exponents at the ordinary surface transition $x_m^s = 1/2$ for $q = 2$ and $x_m^s = 2/3$ for $q = 3$.[14, 16]

The critical corner energy density

$$e_c^{\text{crit}}(N) = e_c^{\text{crit}}(\infty) + A_e(\theta)\, N^{-x_e^c}$$

contains a regular part which depends on the opening angle and the bond orientation. In order to obtain the corner exponent the regular contribution has to be subtracted. This can be done by calculating $e_c^{\text{crit}}(N)$ for

Table I. Scaling Dimension of the Corner Magnetization for the q-State Potts Model as a Function of the Opening Angle[a]

	x_m^c			x_m^c	
θ (deg)	$q=2$	Expected	θ (deg)	$q=3$	Expected
360(d)	0.25(1)	0.25	180(e)	0.667(1)	0.6667
270(c)	0.332(1)	0.333333	90(b)	1.331(3)	1.3333
225(c)	0.400(1)	0.4	53.13(b)	2.243(3)	2.2586
180(e)	0.5000(1)	0.5	45(a)	2.66(1)	2.6667
90(b)	0.999994(6)	1	26.56(a)	4.516(3)	4.5172
53.13(b)	1.693961(7)	1.693955	18.43(a)	6.52(2)	6.5094
45(a)	2.00000(2)	2	14.04(a)	8.53(4)	8.5493
36.87(b)	2.44098(6)	2.441016	11.31(a)	10.58(4)	10.6101
28.07(b)	3.2057(3)	3.205986	9.46(a)	12.66(4)	12.6819
22.62(b)	3.979(4)	3.978804			
11.42(b)	7.8796(6)	7.880092			

[a] The numbers in parentheses give the estimated uncertainty in the last digit. The letters refer to the system shapes in Fig. 2.

either fixed or free boundary conditions at the top edge. The asymptotic value is the same in both cases, but the amplitudes of the finite-size corrections are different. Taking the difference, one obtains

$$\Delta e_c(N) = [A_c^{\text{fixed}}(\theta) - A_c^{\text{free}}(\theta)]\, N^{-x_e^c}$$

Proceeding in this way, one avoids a systematic error, linked with the estimation of the regular part, and the finite-size corrections are amplified because the signs of the amplitudes are different for the two boundary conditions.

The extrapolated values of the finite-size estimates for the corner exponent $x_e^c(\theta)$ are given in Table II. They do not depend on the bond

Table II. As in Table I, for the Corner Energy Density

	x_e^c		
θ (deg)	$q=2$	$q=3$	Expected
180(e)	2.001(1)	2.01(3)	2
90(b)	3.999(1)	4.00(4)	4
45(a)	7.993(7)	8.0(1)	8
26.56(a)	13.52(2)	13.5(1)	13.5516
18.43(a)	19.6(4)	19.7(4)	19.5281

orientation, as expected, and are identical for $q=2$ and $q=3$. This is consistent with the conformal result, since, at the ordinary transition, the surface exponent x_e^s which enters in (1.1) is equal to 2, the dimension of the system, quite generally.[20, 16] The numerical values are in good agreement with the results expected from conformal invariance, too.

The conformal expression for the corner exponent (1.1) only applies to systems where the correlations are isotropic. In the case of an anisotropic system, with a coupling constant ratio $r=K_1/K_2$, the correlation lengths are different and take the values ξ_1 and ξ_2 in the vertical and horizontal directions, respectively. Isotropy can be restored by changing the lattice parameters a_1 and a_2 in such a way that, in the rescaled system, the correlation lengths become the same, i.e., $\xi_1 a_1 = \xi_2 a_2$.[1, 2] As a consequence, one obtains an effective opening angle which, in the geometry of Fig. 2a, is given by

$$\tan\theta_{\text{eff}} = \zeta \tan\theta, \qquad \zeta = \frac{a_2}{a_1} = \frac{\xi_1}{\xi_2} \tag{3.1}$$

where ζ is the anisotropy factor.

For the Potts model, the following form of the anisotropy factor at the critical point has been conjectured:[21]

$$\zeta = \tan\frac{\pi u}{2\lambda}, \qquad \frac{\sin u}{\sin(\lambda-u)} = \frac{x_{1c}}{\sqrt{q}} = \frac{\sqrt{q}}{x_{2c}}, \qquad 2\cos\lambda = \sqrt{q} \tag{3.2}$$

When $q=2$, it reduces to the known exact result $\zeta = \cosh 2K_{1c}/\cosh 2K_{2c}$ for the Ising model.[2]

Table III. Corner Exponents for the Ising Model on an Anisotropic Lattice as a Function of the Anisotropy Ratio r^a

	x_m^c		x_e^c	
r	Numerical	Expected	Numerical	Expected
0.200	4.5737(8)	4.57374	18.2(6)	18.295
0.300	3.595(2)	3.59518	14.36(8)	14.381
0.400	3.05(2)	3.06772	12.24(8)	12.271
0.500	2.7326(1)	2.73264	10.92(5)	10.931
0.600	2.4999(5)	2.49960	9.96(5)	9.998
10.00	1.16(2)	1.16200	4.6(1)	4.648

[a] We used the shape of Fig. 2a with an opening angle $\theta=45°$. The numerical values are compared to the conformal result with a rescaled angle, as explained in the text.

Table IV. As in Table III, for the Three-State Potts Model

	x_m^c		x_e^c	
r	Numerical	Expected	Numerical	Expected
0.109	9.31(3)	9.30667	27(1)	27.920
0.166	6.98(4)	7.00928	21.2(9)	21.028
0.259	5.30(3)	5.31052	15.9(2)	15.931
0.414	4.05(4)	4.05604	12.1(1)	12.168
0.692	3.137(6)	3.13157	9.3(1)	9.365
1.241	2.45(1)	2.45244	7.3(1)	7.357
2.561	1.955(6)	1.95572	5.8(2)	5.867
7.530	1.5(1)	1.59445	4.6(2)	4.783

The corner exponents x_m^c and x_e^c obtained on anisotropic systems with an opening angle $\theta = 45°$ in Fig. 2a and different anisotropy ratio r are given in Tables III and IV. They are in good agreement with the conformal result (1.1) when the opening angle is replaced by its effective value given by (3.1).

4. CONCLUSION

The scaling dimensions of the tip magnetization and energy density at a corner have been calculated for the Ising and three-state Potts models in two dimensions as functions of the opening angle θ. Using transfer operator techniques and finite-size scaling at the critical point, we have tested the result of conformal invariance, predicting a simple relation between corner exponents, surface exponents, and opening angle, for a broad spectrum of θ values. In the case of the Ising model, the magnetization results extend previous studies where simple fractions of π were considered, whereas the energy results are new. Isotropic and anisotropic systems have been treated. In the latter case, the conformal result still applies, provided the opening angle is properly rescaled in order to restore isotropy.

As a possible extension of this work, one may mention the possiblity to consider the same problem for noninteger values of q, using the relation of the Potts model with either Withney polynomials[22] or ice-rule vertex models.[23, 24]

ACKNOWLEDGMENTS

P.L. thanks the Hungarian Soros Foundation for a travel grant. This work was supported by CNIMAT under project 155C96 and by the Hungarian National Research Fund under grant OTKA TO12830.

REFERENCES

1. J. L. Cardy, *J. Phys. A* **16**:3617 (1983).
2. M. N. Barber, I. Peschel, and P. A. Pearce, *J. Stat. Phys.* **37**:497 (1984).
3. I. Peschel, *Phys. Lett.* **110A**:313 (1985).
4. C. Kaiser and I. Peschel, *J. Stat. Phys.* **54**:567 (1989).
5. B. Davies and I. Peschel, *J. Phys. A* **24**:1293 (1991).
6. D. B. Abraham and F. T. Latrémolière, *Phys. Rev. E* **50**:R9 (1994).
7. D. B. Abraham and F. T. Latrémolière, *J. Stat. Phys.* **81**:539 (1995).
8. C. Kaiser and I. Peschel, *J. Phys. C* **6**:1149 (1994).
9. A. J. Guttmann and G. M. Torrie, *J. Phys. A* **17**:3539 (1984).
10. J. L. Cardy and S. Redner, *J. Phys. A* **17**:L933 (1984).
11. B. Duplantier and H. Saleur, *Phys. Rev. Lett.* **57**:3179 (1986).
12. D. Considine and S. Redner, *J. Phys. A* **22**:1621 (1989).
13. C. Vanderzande, *J. Phys. A* **23**:563 (1990).
14. J. L. Cardy, *Nucl. Phys. B* **240**:514 (1984).
15. I. Peschel, L. Turban, and F. Iglói, *J. Phys. A* **24**:L1229 (1991).
16. F. Iglói, I. Peschel, and L. Turban, *Adv. Phys.* **42**:683 (1993).
17. L. Mittag and M. J. Stephen, *J. Math. Phys.* **12**:441 (1971).
18. F. Y. Wu, *Rev. Mod. Phys.* **54**:235 (1982).
19. M. Henkel and G. Schütz, *J. Phys. A* **21**:2617 (1988).
20. T. W. Burkhardt and J. L. Cardy, *J. Phys. A* **20**:L233 (1987).
21. D. Kim and P. A. Pearce, *J. Phys. A* **20**:L451 (1987).
22. H. W. J. Blöte and M. P. Nightingale, *Physica* **112A**:405 (1982).
23. H. N. V. Temperley and E. H. Lieb, *Proc. R. Soc. Lond. A* **322**:251 (1971).
24. R. J. Baxter, S. B. Kelland, and F. Y. Wu, *J. Phys. A* **9**:397 (1976).